

Low-Light Image Enhancement via Mixture L2-LP Variational Retinex Model with Adaptive Texture Map

Thesis Supervisor
Prof. Youji Iiguni

Kazuki Kurihara

Division of Systems Science and Applied Informatics
Department of Systems Innovation
Graduate School of Engineering Science
Osaka University

January 28, 2020

Abstract

The methods of low-light image enhancement have been paid attention to with the wide spread of computer vision applications used in outdoors. Many methods have used cost functions which are based on Retinex theory that decomposes an observed image into reflectance and illumination. However, the enhanced image causes negative effects such as halo artifacts, noise amplification, and over-enhancement when the methods can not sufficiently consider the characteristics of reflectance and illumination. Thus, in order to alleviate such effects, we incorporate constraint terms which further consider the characteristics of reflectance and illumination with a cost function. In addition, we develop an adaptive texture map as a weight of the constraint term on reflectance, which is used to tune noise reduction rate according to brightness of an observed image. Moreover, the adaptive texture map contributes to reveal fine textures detail in the estimated reflectance. Both qualitative and quantitative evaluations show that the proposed method can sufficiently enhance low-light images while suppressing halo artifacts, noise amplification, and over-enhancement.

Contents

1	Introduction	1
2	Related Work	3
2.1	Retinex Theory	3
2.2	Variational Retinex Model	4
2.3	Local Variation Deviation	5
2.4	Consideration of Problems	6
3	Proposed Method	9
3.1	Mixture L2-LP Variational Model	9
3.2	Adaptive Texture Map	11
3.3	Solution	13
4	Experiment	19
4.1	Testing Datasets	19
4.2	Competing Methods	19
4.3	Decomposition Comparison	20
4.4	Qualitative Evaluation	22
4.5	Quantitative Evaluation	22
4.6	Parameter Study	27
5	Conclusion	31

Chapter 1

Introduction

Images captured under low light conditions suffer from poor visibility, low contrast, and unexpected noise. Consequently, low-light images prevent human from extracting hidden meaningful information. Moreover, such degradation affect vision techniques, including consumer digital cameras, mobile phones and video surveillance systems, which can be often used in outdoors. Therefore, the methods of low-light image enhancement, including histogram equalization (HE) algorithms [1] - [3], dehaze-based algorithms [4], [5], and Retinex-based algorithms[6] - [12] have been proposed to deal with above problems.

HE algorithms are probably the most intuitive and simplest way to improve image contrast. The operation stretches the dynamic range of intensity level of an observed image. As a result, the methods tend to result in over-enhancement. In addition, the methods can not consider the intensive noise hidden under dark regions in low light images. Therefore, the methods lead to noise amplification after contrast enhancement.

Some methods [4], [5] noticed that the inverted low-light images look like haze images. According to this observation, the methods attempted to deal with low-light images. Although the methods can obtain reasonable results, they do not provide a sufficient physical explanation for the basic model. Many methods that focus on Retinex theory, which is a color perception model based on human visual system, have been proposed for low-light image enhancement. According to the basic assumption of Retinex theory [13], an observed image can be decomposed into two parts: reflectance and illumination. Early attempts in this theory, such as Single-Scale Retinex (SSR) [6] and Multi-Scale Retinex (MSR) [7], treat reflectance as the enhancement result. However, the methods cause over-enhancement and generate unrealistic result. This problem is mainly caused by the logarithmic operation when enhancing a low-light image. To overcome this problem, Fu proposed a simultaneous reflectance and illumination estimation (SRIE) [8] and a weighted variation model (WVM) [9]. The methods demonstrated that the linear domain model is better than the log-transformed domain in preserving naturalness. These methods have good performances in the enhancement, but they still have the problem that noise is quite observable in the results, especially when an observed image has much noise in dark regions. Cai *et al.* [11] proposed a Joint intrinsic-extrinsic Prior (JieP) model for Retinex decomposition by considering the properties of 3D objects. The method can significantly distinguish between texture and structure regions and estimate illumination while keeping the structure information. However, the method generates noise amplification in dark regions, since the method can not sufficiently consider the constraint term on reflectance. Li

presented a robust Retinex model (RRM) [12] by adding a noise term to the cost function in order to deal with noise amplification due to the estimation errors. RRM effectively suppresses noise amplification, but the method has difficulty balancing piece-wise smoothed illumination and details of reflectance. Many above methods adopt a L_1 norm to the constraint term on reflectance, but the tiny details of the estimated reflectance are susceptible to be damaged. Moreover, by adopting a L_2 norm to the constraint term on illumination, the estimated illumination is over-smoothed without keeping the structure information.

In this paper, we propose a new cost function that further considers the characteristics of both reflectance and illumination. We adopt L_2 and L_p norms to the constraint terms on reflectance and illumination in order to preserve fine textures detail as much as possible, and smooth illumination as as much as possible while keeping the structure information. Moreover, we introduce an adaptive texture map into a weight of the constraint term on reflectance. The adaptive texture map is used to tune a noise reduction rate according to brightness of an observed image. In addition, the adaptive texture map contributes to reveal fine textures detail in the estimated reflectance. Finally, we show that the proposed method outperforms the state-of-the-art methods in both qualitative and quantitative evaluations.

Chapter 2

Related Work

In this section, we describe a well-known theory in image enhancement. Next, we introduce the conventional methods that apply this theory to the optimization equations with the cost functions. Finally, we consider various problems in the methods.

2.1 Retinex Theory

The Retinex theory [13] is a color perception model based on human visual system. The model decomposes an observed image into reflectance and illumination as follows:

$$S = R \circ I, \quad (2.1)$$

where S is an observed image, R and I represent reflectance and illumination, respectively. The operator “ \circ ” denotes the element-wise multiplication. As shown in Fig.2.1, reflectance represents the intrinsic characteristics of the object and contains rich textures details. On the contrary, illumination represents the extrinsic property and contains the structure information. The conventional Retinex-based enhancement methods such as [6], [7] are defined as

$$\log R = \log S - \log [G * S], \quad (2.2)$$

where “ $*$ ” represents the convolution operator, and G is the Gaussian low-pass filter. This method assumes that illumination can be estimated by passing an observed image through the Gaussian low-pass filtered version of the image. Moreover, reflectance is computed

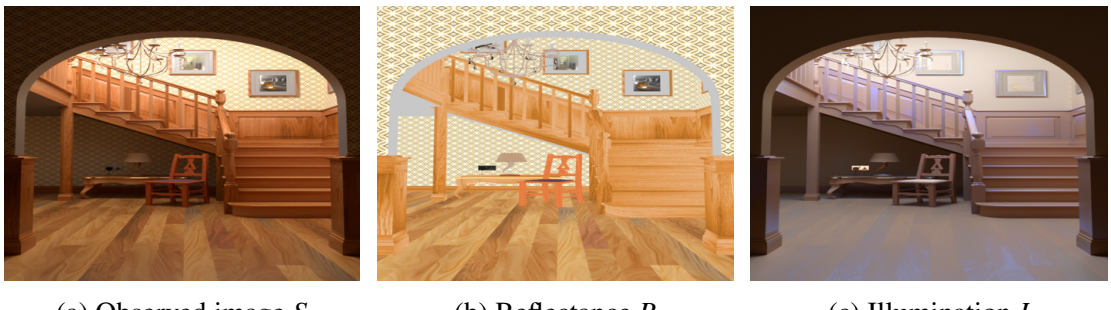
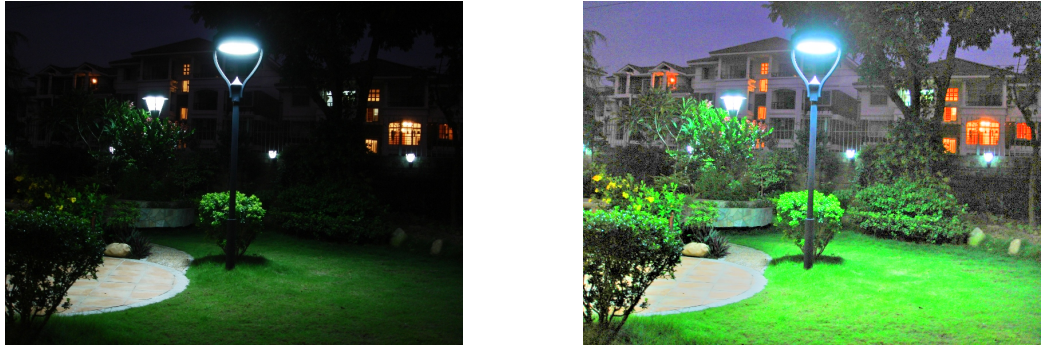


Figure 2.1: The images based on the Retinex theory [16].



(a) Observed image S

(b) Reflectance R

Figure 2.2: The results of the conventional Retinex-based enhancement method [7].

by subtracting the estimated illumination from an observed image. However, this method generates halo artifacts around the edges of object when the size of the Gaussian low-pass filter is not appropriate. In addition, as shown in Fig.2.2, this method causes over-enhancement and much noise in the estimated reflectance.

2.2 Variational Retinex Model

Various methods have proposed optimization problems based on the Retinex theory in order to estimate reflectance and illumination efficiently. The methods introduce constraint terms on reflectance and illumination which consider the characteristics for them into the optimization problems. The methods usually adopt L_1 and L_2 norms to the constraint terms. For example, Fu [8] proposed the following cost function which minimizes the optimization problem:

$$\begin{aligned} & \arg \min_{R,I} E(R,I) \\ & E(I,R) = \|R \circ I - S\|_2^2 + \alpha \|\nabla I\|_2^2 + \beta \|\nabla R\|_1 + \gamma \|I - I_0\|_2^2 \\ & \text{s.t. } S \leqq I, \end{aligned} \tag{2.3}$$

where α , β , γ are three positive parameters, and I_0 is the enhanced illumination using gamma correction. The first term $\|R \circ I - S\|_2^2$, which corresponds to L2 data fidelity, is to minimize the distance between the estimated ($R \circ I$) and an observed image S . The second term $\|\nabla I\|_2^2$ enforces spatially smoothness on the illumination I . The third term $\|\nabla R\|_1$, which corresponds to TV reflectance sparsity, enforces piece-wise continuous on the reflectance R . The last term $\|I - I_0\|_2^2$, which penalizes the brightness of illumination component, is used to avoid a scaling problem.

This method was implemented with a linear domain. As a result, this method can preserve more naturalness than the methods implemented with a log-transformed domain. As shown in Fig.2.3, this method employs the fourth term which minimizes the difference between I and I_0 for the sake of suppression of over-enhancement in the estimated reflectance. Moreover, this method can suppress noise amplification due to the L_1 norm constraint term on reflectance in the estimated reflectance.

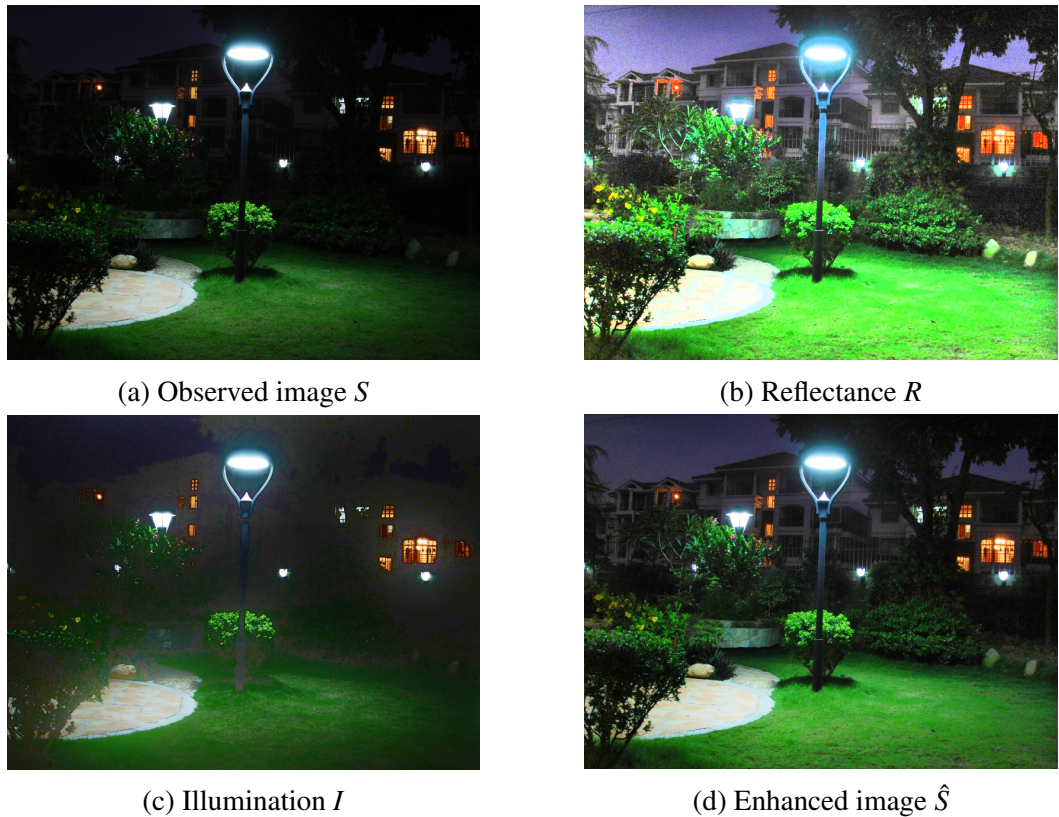


Figure 2.3: The results of SRIE [8].

2.3 Local Variation Deviation

This section discusses edge/structure preserving image smoothing and a joint intrinsic-extrinsic prior model (JieP) which are proposed by Cai [11]. This model adopted the image smoothing function as the constraint term on illumination in Eq.(2.3).

In statics, the standard deviation represents a measure to quantify the consistency of a set of data. The local variation deviation (LVD) is used to identify different type of the variation with the statistical property. By using the feature in terms of image analysis, the LVD can surprisingly distinguish between texture and structure regions, since texture component includes weak correlation and structure component includes strong correlation.

The \mathcal{R}_d denotes a relative LVD extracted from I :

$$\mathcal{R}_d = \left| \frac{\nabla_d I}{\frac{1}{|\Omega|} \sum_{\Omega} \nabla_d I + \varepsilon} \right|, \quad (2.4)$$

where ∇_d is the horizontal and vertical ($d \in h, v$) gradient operator, Ω is the local patch size ($r \times r$), and ε is a small number to avoid division by zero. The edge/structure preserving smoothing property of the LVD can be explained intuitively as follows: (In the following, the mean local variation means $\bar{\nabla}I = \frac{1}{|\Omega|} \sum_{\Omega} \nabla I$):

- **Case1: Flat.** If the value of the patch I is almost constant, $\nabla I \approx 0$ and $\bar{\nabla}I \approx 0 \rightarrow \mathcal{R} \approx 0$.

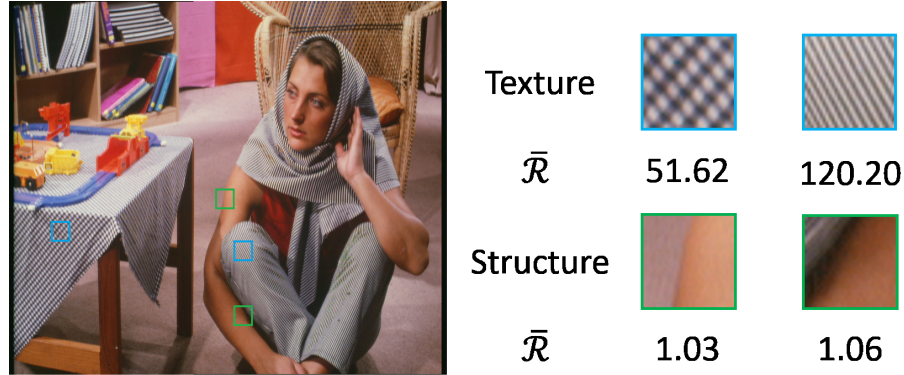


Figure 2.4: The analysis of the local variation deviation for different patches. \bar{R} is the average of variation deviation in the local patches. The local variation deviation surprisingly distinguish textures (blue squares) and structures (green squares).

- Case2: **Texture.** If the value of the patch I changes frequently, ∇I varies more rapidly than $\bar{\nabla}I \rightarrow \bar{R} \gg 1$.
- Case3: **Structure.** If the value of the patch I changes in accordance with structure, the deviation of ∇I fluctuates small $\rightarrow \bar{R} \approx 1$.

To quantitatively analyze the effectiveness of the distinction of the LVD measure, we evaluated the average values of the LVD in the local patches in both texture and structure regions. Fig.2.4 summarizes the result of this analysis. The blue squares represent texture regions and the green squares represent structure regions. We can see that there is a clear difference between texture and structure regions. In order to take the effectiveness of the LVD into consideration, Cai replaced the constraint term on illumination by a L_1 norm constraint term of the LVD in a cost function to minimize an optimization problem. The function is formulated as follows:

$$E(I, R) = \|R \circ I - S\|_2^2 + \alpha \left\| \frac{\nabla I}{\frac{1}{\Omega} \sum_{\Omega} \nabla I + \varepsilon} \right\|_1 + \beta \|\nabla R\|_1 + \gamma \|I - B\|_2^2, \quad (2.5)$$

where α, β, γ are three positive parameters and B ($B = \max_{\Omega}(\max_{c \in \{r,g,b\}} S_c)$) represents the bright channel prior (BCP) of an observed image S . As shown in Fig.2.5, the estimated illumination removes texture component while preserving the structure information. Thus, in the estimated reflectance, JieP significantly suppresses the awareness of halo artifacts along with edge regions. Moreover, more textures details are revealed in the estimated reflectance.

2.4 Consideration of Problems

Fu *et al.* and Cai *et al.* can enhance low-light images by solving each minimization optimization problem. However, the methods have some problems in the enhanced image or the estimated component. Therefore, this section discusses such problems by using Fig.2.6.

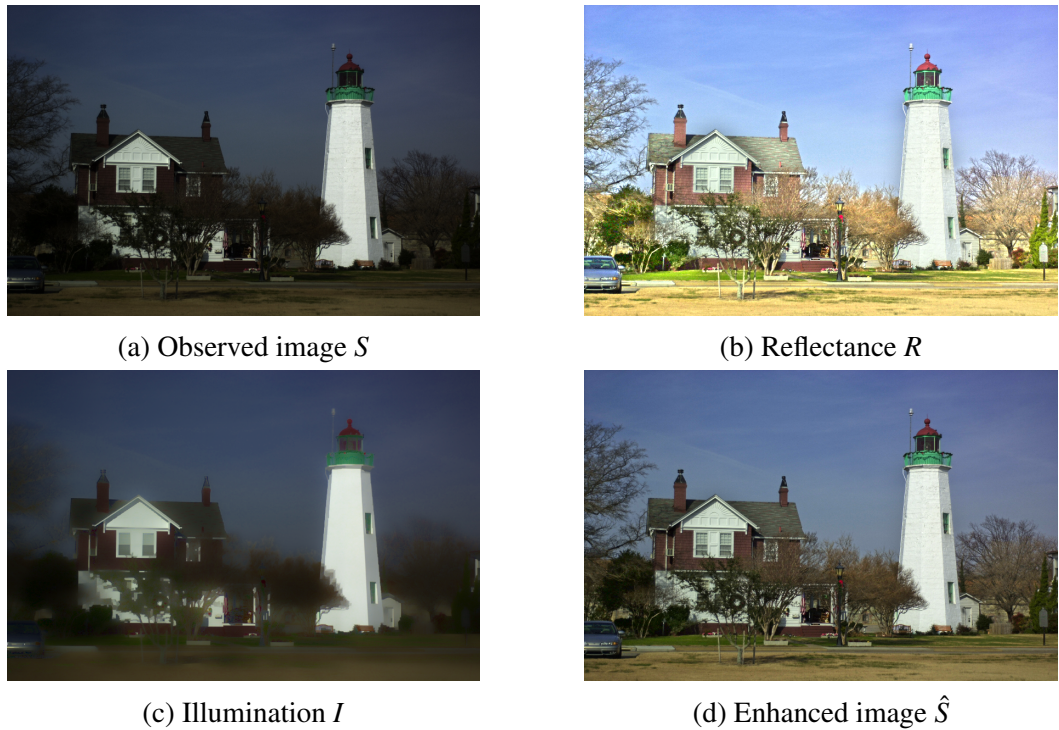


Figure 2.5: The results of JieP [11].

- **SRIE** is prone to over-smooth illumination without preserving the structure information, because the L_2 constraint term is based on the assumption that illumination should be spatially smooth. As a result, as shown in Fig.2.6a, the estimated reflectance generates halo effect along with edge regions that have large intensity gradient. Moreover, as can be seen in Fig.2.3b, in the estimated reflectance, much noise remain in dark regions and over-enhancement causes in bright regions because the constraint term on reflectance is lack of a weight to distinguish between dark and bright regions.
- **JieP** can significantly take consideration of the constraint term on illumination, but is not sufficient for reflectance. Therefore, as can be seen in Fig.2.6b, the estimated reflectance amplifies noise in dark regions and is over-enhanced in bright regions. Moreover, the constraint term on illumination adopts the L1 norm, so that the method may damage the structure information too much in the estimated illumination.



(a) Reflectance (SRIE)



(b) Reflectance (JieP)

Figure 2.6: Each problem which SRIE and JieP cause in the estimated reflectance.

Chapter 3

Proposed Method

This section discusses the proposed method which conquers the problems described in Sec.2.4. First, we introduce a mixture L_2 - L_p variational retinex model which further considers the characteristics of reflectance and illumination in Sec.3.1. Next, we develop an adaptive texture map which tunes the noise reduction rate according to the brightness of an observed image and texture component in reflectance in Sec.3.2. Finally, we mention a solution of the proposed minimization optimization problem in Sec.3.3.

Fig.3.1 shows the flowchart of the proposed method. To explain the flow of the proposed method briefly, the proposed method obtains a low-light image and an initialized illumination which is called the bright channel prior. Next, the proposed method converts a low-light image to HSV-color space and extract only value (V) channel. The proposed method obtains reflectance and illumination which meet the appropriate constraints for them by iteratively solving sub-problems related with reflectance and illumination. Finally, the proposed method multiples the estimated reflectance and the estimated illumination, converts the obtained enhanced image to RGB-color space.

3.1 Mixture L2-LP Variational Model

The conventional methods adopt a L_1 norm to the constraint term on reflectance, but the fine details of the estimated reflectance are susceptible to be damaged. Furthermore, by adopting a L_2 norm to the constraint term on illumination, the estimated illumination loses the structure information due to over-smoothing. Therefore, the proposed method introduces L_2 and L_p norm into the constraint terms on reflectance and illumination in a cost function. As a result, the proposed method can preserve fine textures detail as much as possible in the reflectance estimation, and keep the structure information as much as possible while avoiding the texture-copy problem in the illumination estimation. Thus, we formulate the proposed cost function of the minimization optimization problem as:

$$\begin{aligned} & \arg \min_{R,I} E(R,I) \\ E(I,R) = & \|R \circ I - S\|_2^2 + \alpha \left\| \frac{\nabla I}{\frac{1}{|\Omega|} \Sigma_Q \nabla I + \varepsilon} \right\|_p^p + \beta \|W \circ \nabla R\|_2^2 + \gamma \|I - B\|_2^2, \end{aligned} \quad (3.1)$$

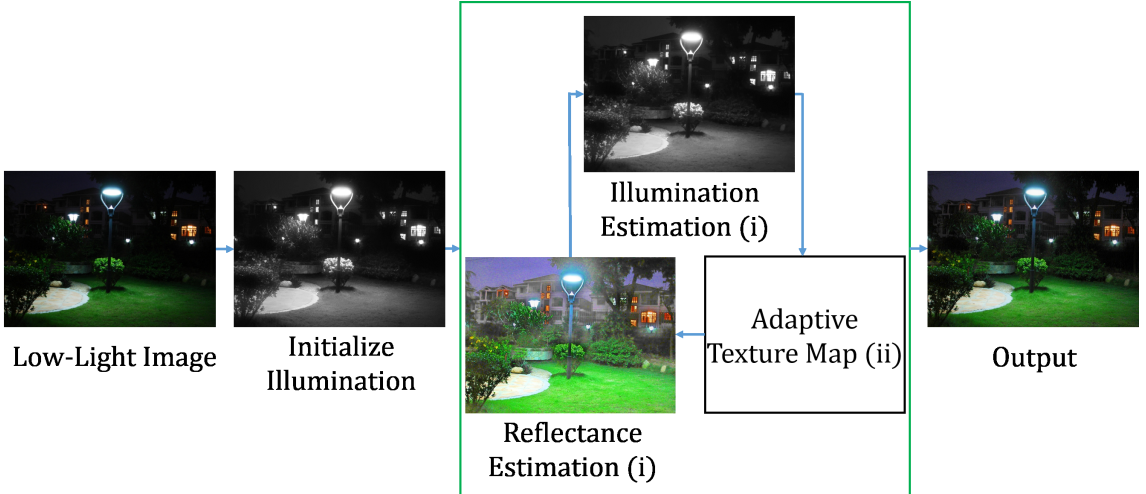


Figure 3.1: Flowchart of the proposed method. (i)The proposed method changes the constraint terms which further considers the characteristics for reflectance and illumination. (ii)The proposed method develop an adaptive texture map as a weight of the constraint term on reflectance which tunes the noise reduction rate according to the brightness of an observed image and texture component in reflectance.

where $\|\cdot\|_p$ denotes the L_p norm constraint term ($0 \leq p \leq 2$), and W is the adaptive texture map which tunes the noise reduction rate according to the brightness of an observed image and texture component in reflectance.

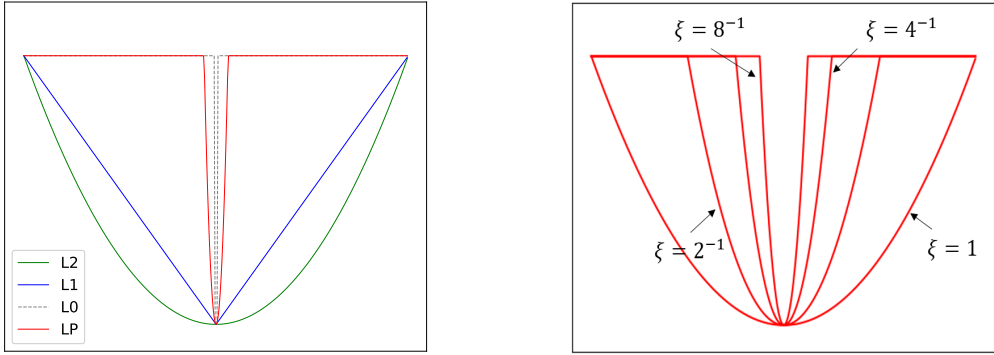
As described in [15], a block coordinate descent method [17] is used in order to find an optimal solution to the non-convex objective Eq.(3.1). Since the L_p norm constraint term causes non-smooth optimization, the proposed method adopts an iteratively re-weighted least square (IRLS) method [18] and rewrite the second term in Eq.(3.1) as:

$$\left\| \frac{\nabla I}{\frac{1}{|\Omega|} \Sigma_{\Omega} \nabla I + \varepsilon} \right\|^p = \|U \circ \nabla I\|^2, \quad (3.2)$$

$$U = \begin{cases} \frac{1}{\xi^{2-p}}, & \left| \frac{\nabla I}{\frac{1}{|\Omega|} \Sigma_{\Omega} \nabla I} \right| < \xi \\ \frac{\left| \frac{1}{|\Omega|} \Sigma_{\Omega} \nabla I \right|^{2-p}}{|\nabla I|^{2-p}} \frac{1}{|\Sigma_{\Omega} \nabla I|^2}, & \text{otherwise} \end{cases}$$

$$= \begin{cases} \frac{1}{\xi^{2-p}}, & \left| \frac{\nabla I}{\frac{1}{|\Omega|} \Sigma_{\Omega} \nabla I} \right| < \xi \\ \frac{1}{\left| \frac{1}{|\Omega|} \Sigma_{\Omega} \nabla I \right|^p |\nabla I|^{2-p}}, & \text{otherwise} \end{cases}, \quad (3.3)$$

where U is a weight matrix to approximate the L_0 norm function by using a L_2 norm format based on [19]. As can be seen in Fig.3.2a, the red curve can approximate the most sparse L_0 function. Therefore, the proposed method can remove fine textures detail and preserve meaningful salient structures in the estimated illumination. As shown in Fig.3.2b, with the decease of the value ξ , the L_p norm function is getting close to the L_0 function. Therefore, as the value of ξ is getting large, the more convex-like the L_p norm function



(a) Plots of different penalty functions (b) Plots of L_p norm for different values p

Figure 3.2: Plots of the analysis of the L_p norm function when $p = 0$.

is. In addition, it is easier to optimize the cost function. In contrast, as the value of ξ is getting small, the more steep the L_p norm function is. Therefore, it is more difficult to optimize cost function.

Fig.3.3 shows the effect of changing the value of p in the range ($0 \leq p \leq 2$) in the estimated illumination. As the value of p decreases, the estimated illumination becomes smooth and texture-less, while the estimated reflectance contains more rich textures detail. In particular, when $p = 0$, some salient structure information in the estimated illumination may be lost too much, because the L_0 norm has strong sparsity.

3.2 Adaptive Texture Map

This section discusses the effect of an adaptive texture map using as a weight of the constraint term on reflectance. As discussed in Sec.2.1, reflectance component contains rich details. However, when a low-light image is enhanced, noise hidden in dark regions is amplified and over-enhancement is caused in bright regions. Therefore, the constraint term on reflectance requires the weight which tunes the noise reduction rate according to the brightness of an observed image. In addition, the preferable reflectance's gradients should be smooth in homogeneous regions while should be preserved edges and textures details. Thus, when estimating reflectance, the weight which can recognize more texture regions is required so that the estimated reflectance is not damaged at texture regions. Fig.3.4 shows the summary of the above discussion. Then, the adaptive texture map W is set so that the third term in Eq.3.1 performs strong noise reduction in dark and homogeneous regions, while it performs weak noise reduction in bright and texture regions. Such a map W is formulated as:

$$W_d = W_B \circ A_d, \quad (3.4)$$

where d represents horizontal (h) and vertical (v) directions, and W_B represents an initial estimated weight map by inverting the normalized bright channel of an observed image, and A_d represents a texture map that effectively distinguishes between homogeneous and texture regions.

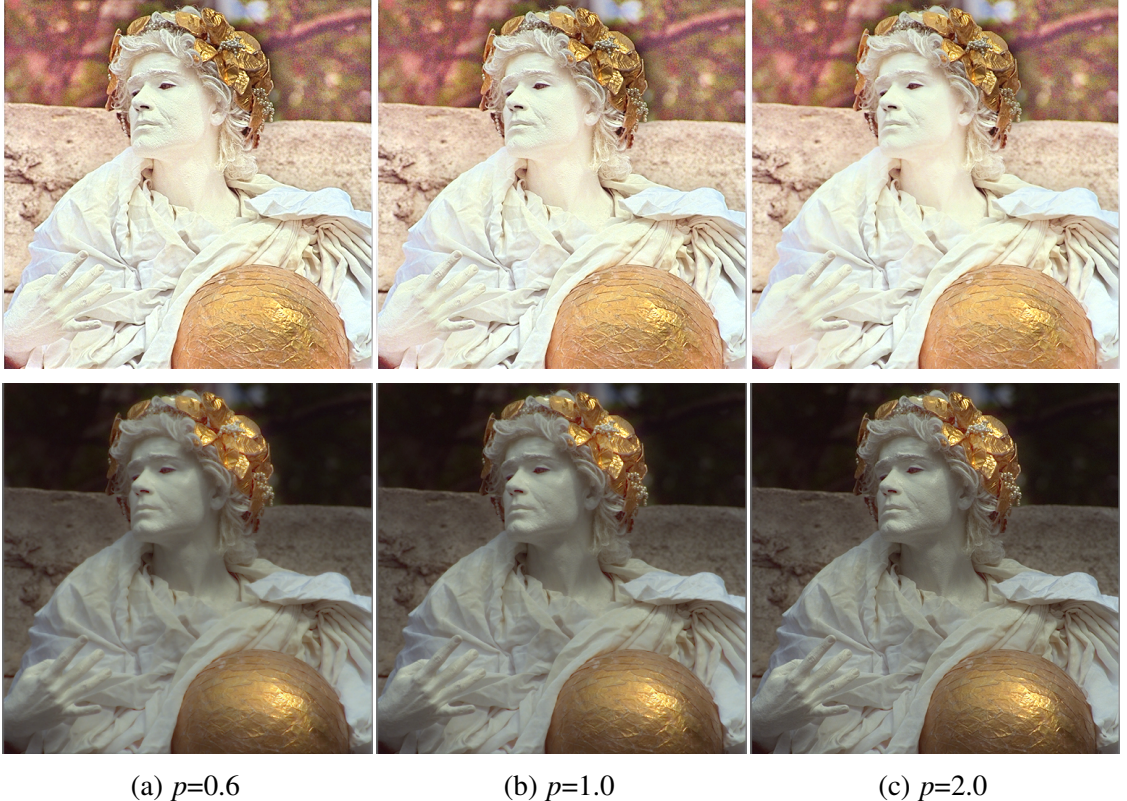


Figure 3.3: Comparison of decomposition results for different values of norm p . ((a)-(c) top: reflectance, bottom: illumination)

In the same way as in [21], given an observed low-light image, W_B should selectively assigns different values to dark and bright regions according to BCP since the estimated bright channel contains small values in dark regions and vice versa. Thus, W_B is given as:

$$W_B = 1.0 - \max_{c \in \{r,g,b\}} S^c. \quad (3.5)$$

Fig.3.5 shows the image of W_B . Since larger weight values are assigned in dark regions, W_B performs a stronger noise reduction. In contrast, a weaker noise reduction is performed in bright regions by W_B .

Moreover, the texture map A_d is set as the inverse of the a_r -th power of the absolute value of a mean local variation (MLV) [11], so that it can significantly distinguish between homogeneous regions and texture regions:

$$A_d = \frac{1}{\left| \frac{1}{|\Omega|} \sum_{\Omega} \nabla_d R \right|^{a_r} + \epsilon}, \quad (3.6)$$

where $a_r (0 \leq a_r \leq 1)$ is an exponential parameter to adjust the awareness of textures detail for reflectance. As shown in Fig.3.6a and 3.6b, when $a_r = 1.0$, the texture map A_d extracts salient edges but little texture component. In contrast, when $a_r = 0.5$, the texture map extracts both salient edges and rich texture component, but the map amplifies details in flat and homogeneous regions. Therefore, the exponential parameter a_r should be set small in



Figure 3.4: Classification of regions where the adaptive texture map has an impact on.

salient edges and textures details, and set large in flat and homogeneous regions, so that

$$a_r = 1.0 - |\nabla_d R| \exp(1.0 - |\nabla_d R|). \quad (3.7)$$

Fig.3.6c shows the proposed MLV of reflectance. The regions of edges and textures detail are getting revealed and the flat and homogeneous regions are controlled. Therefore, using the texture map, W performs the weaker noise reduction in both edges and texture regions, while performs the stronger noise reduction in homogeneous regions.

The discussion centers on the effectiveness of the adaptive texture map using Fig.3.7. As shown in the yellow and green squares, the estimated reflectance with W can suppress noise amplification in dark regions and over-enhancement in bright regions more than without W . This is because W_B can effectively assign different values between dark and bright regions. Next, in order to confirm the effectiveness of the texture map A_d , the edge magnitude in the red square is calculated:

$$M(h, v) = \sqrt{G_h^2 + G_v^2}, \quad (3.8)$$

where G_h and G_v represent the horizontal and vertical gradient images, respectively. Fig.3.8 shows the plots of average v-axis edge magnitude. It can be seen that the average gradient magnitude with W has larger values and the values fluctuate more rapidly than the ones without W . Therefore, the texture map A_d contributes to the awareness of textures in the estimated reflectance.

3.3 Solution

The optimization problem (3.1) can be solved by iteratively updating sub-problems for reflectance and illumination. In particular, for the k -th iteration of sub-problems:

- 1). **I sub-problem:** Collecting the terms related to I leads to the following sub-problem in (3.1):

$$I_k = \arg \min_I \|R_{k-1} \circ I - S\|_2^2 + \alpha \|U \circ \nabla I\|_2^2 + \lambda \|I - B\|_2^2. \quad (3.9)$$



Figure 3.5: The image of W_B . W_B contains larger values in dark regions, while contains smaller values in bright regions, while contains larger values in dark regions.

The sub-problem (3.9) results in a classic least square problem:

$$i_k = \arg \min_i \|r_{k-1}i - s\|_2^2 + \alpha \|uD_i\|_2^2 + \lambda \|i - b\|_2^2, \quad (3.10)$$

where i is the vectorized format of I and D contains D_h and D_v , which are the Toeplitz matrices obtained from the discrete gradient operators with forward difference. The same notation is used for other matrices (r , s , b corresponds to R , S , and B , respectively). By differentiating the function (3.10) with respect to i , and setting the derivative to 0, we have the following solution:

$$i_{k+1} = (r_{k-1}r_{k-1}^T + \alpha D^T uD + \lambda I)^{-1}(r_{k-1}^Ts + \lambda b). \quad (3.11)$$

Then, the obtained i_k is reformulated into matrix format I_k .

- 2). **R sub-problem:** After acquiring I_k from the above solution, the sub-problem in (3.1) related to R becomes similar to that of I :

$$R_k = \arg \min_R \|R \circ I_k - S\|_2^2 + \beta \|W \circ \nabla R\|_2^2. \quad (3.12)$$

In the same way as in the former derivation, the solution of R is provided as follows:

$$r_k = \arg \min_r \|ri_k - s\|_2^2 + \beta \|wDr\|_2^2, \quad (3.13)$$

$$r_k = (i_k i_k^T + \beta D^T wD)^{-1}(i_k^T s). \quad (3.14)$$

Similarly, the obtained r_k is reformulated into matrix format R_k .

The values of I and R are updated until $\|I_k - I_{k-1}\|/\|I_{k-1}\| \leq \epsilon$ and $\|R_k - R_{k-1}\|/\|R_{k-1}\| \leq \epsilon$ are simultaneously satisfied. After the estimation of reflectance and illumination, a Gamma correction operation is adopted to adjust illumination. Therefore, the final enhanced image is given as $S_{enhanced} = R \circ I^{\frac{1}{\gamma'}}$, where the empirical parameter γ' is set as 2.2. To preserve color information, the Gamma correction is performed in the HSV-color space. Fig.3.9 shows the result of the proposed method. The proposed method can smooth illumination as much as possible while keeping the meaningful structure information in

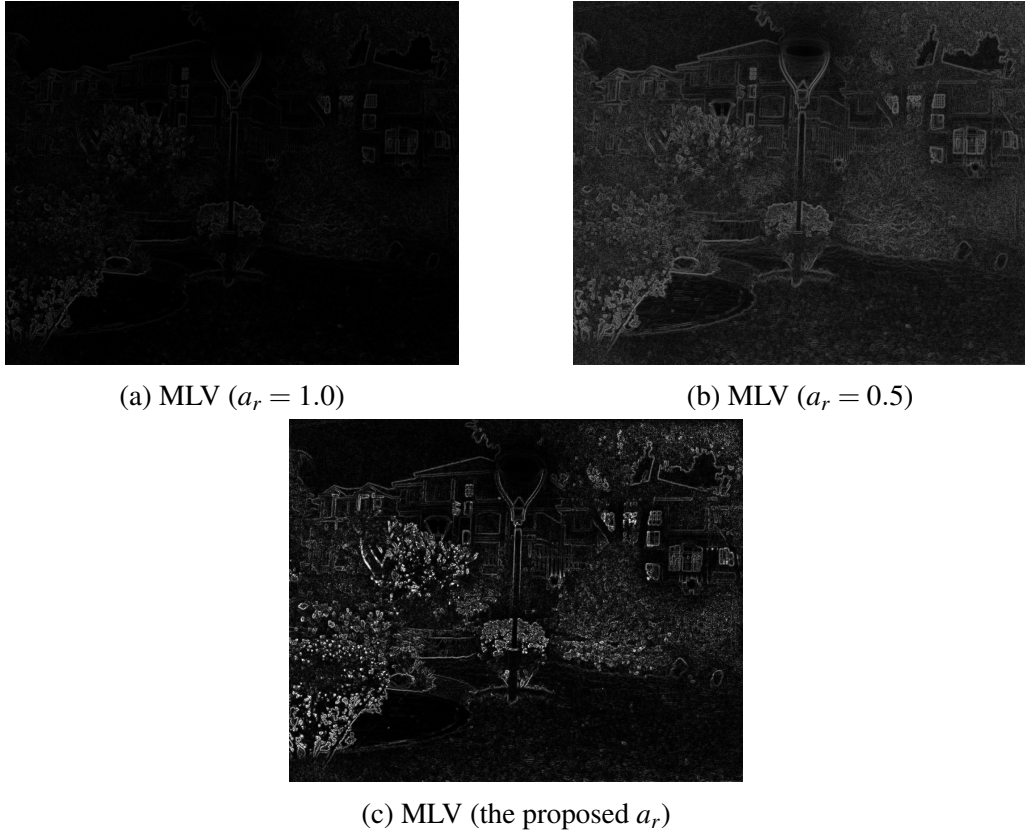


Figure 3.6: Comparison of MLV results for different values of a_r . The proposed a_r contributes to distinguish between regions which should be revealed and regions which should be constrained.

the illumination estimation, and clarify fine textures detail as much as possible while suppressing noise amplification in dark regions and over-enhancement in bright regions in the reflectance estimation. Therefore, we can see that the proposed method naturally enhances low-light images.

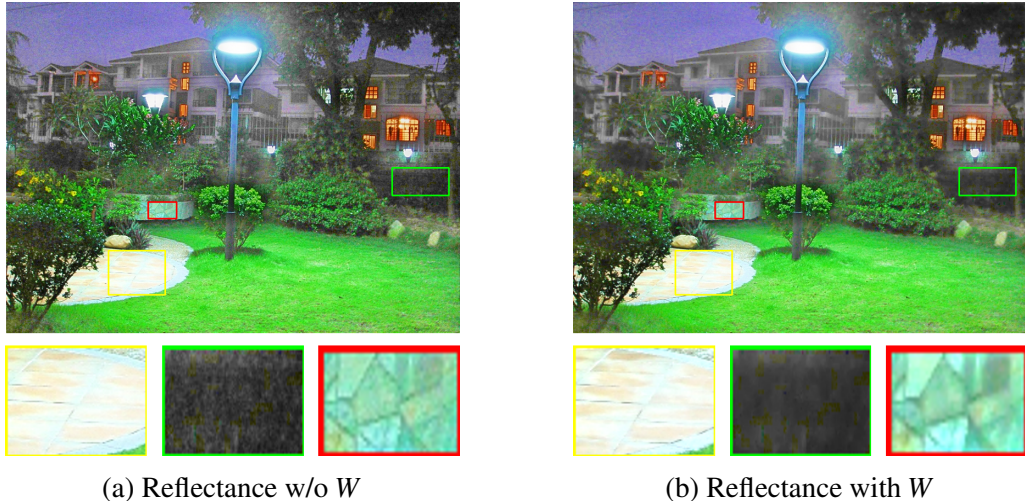


Figure 3.7: Comparison of reflectance results. (a) the estimated reflectance without W ; (b) the estimated reflectance with W .

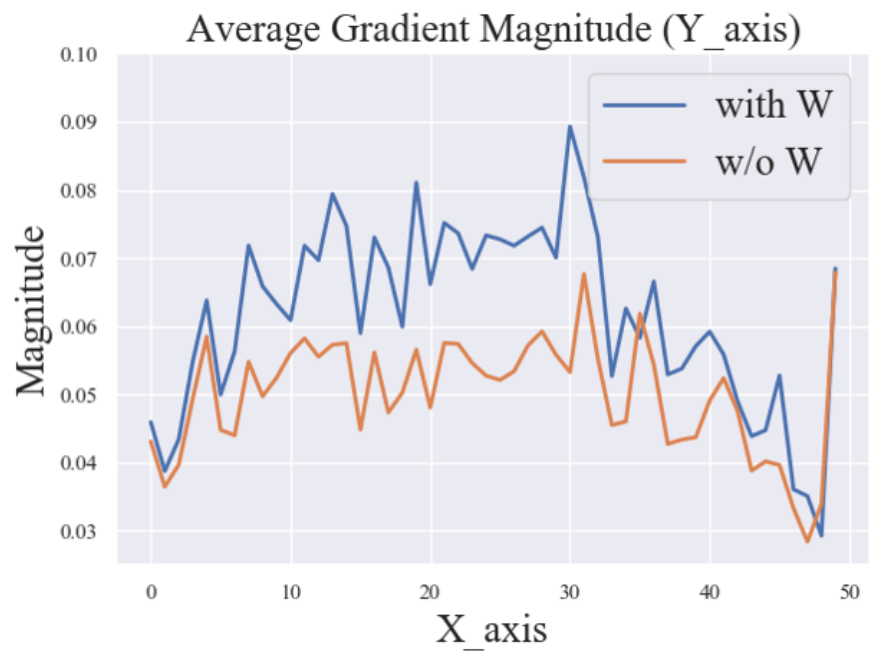


Figure 3.8: Plots of the average edge magnitude.



(a) Low-Light Image



(b) Illumination



(c) Reflectance



(d) Enhanced Image

Figure 3.9: The results of the proposed method.

Chapter 4

Experiment

This section is devoted to demonstrate the superiority of the proposed method in terms of whether the proposed method can further incorporate the characteristics of reflectance and illumination with the cost function of the minimization optimization problem, and whether it can naturally enhance low-light images. The word "naturally" means that the methods can suppress over-enhancement and noise amplification when enhancing. To this aim, this section is composed of the subsequent six aspects: testing datasets, competing methods, decomposition comparison, qualitative evaluation, quantitative evaluation, and parameter study. In this experiment, the empirical parameters are set $\alpha = 0.01$, $\beta = 0.01$, $\gamma = 0.25$, $\varepsilon = 10^{-2}$. In addition, the proposed method is performed on Python implementation on PC with 16GB RAM, Intel Core i7-6700 CPU @ 3.40GHz.

4.1 Testing Datasets

Since we can not obtain the ground truth for low light images in actual applications, we selected 21 image datasets among many datasets which various researches [9], [10], [11] on low-light image enhancement have employed. Fig.4.1 shows the datasets used in the following experiment. The images contain different scenes, such as statue, buildings, Street lamps, landscape, people, sunset, and etc.

4.2 Competing Methods

In this research, five state-of-the-art methods are collected, which can be divided into two types. The first type is composed of Retinex-based model, namely simultaneous reflectance and illumination estimation (SRIE) [8], a weighted variational model (WVM) [9], a robust Retinex model (RRM) [12], and a joint intrinsic-extrinsic prior (JieP) [11]. These methods are based on variational Retinex model, and can simultaneously estimate reflectance and illumination. In addition, SRIE, WVM, and JieP are performed on HSV-color space as well as the proposed method. The second type is composed of non-Retinex model, namely low-light image enhancement via illumination map estimation (LIME) [10]. This method is based on dehazing model and enhances low-light images by estimating the transmission map using the energy function. Programming codes of all methods are downloaded from the author's websites such as Github and implemented with the



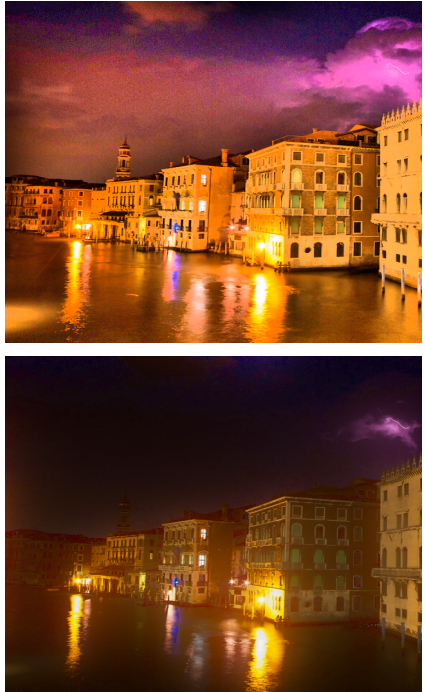
Figure 4.1: 21 image datasets which are captured at diversified locations.

recommended experimental settings.

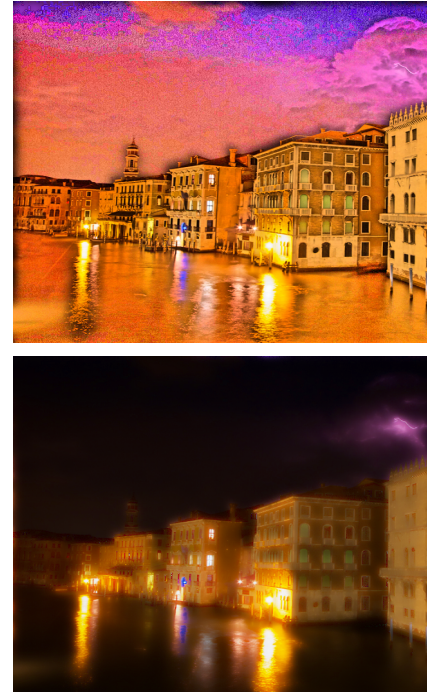
4.3 Decomposition Comparison

The aim of this section is to evaluate how accurately the proposed method estimates reflectance and illumination. It is assumed in [13] that illumination should not distort the structure information while keeping smoothness, and reflectance should contain rich detail of an observed image. Negative effects such as halo artifacts, noise amplification, and over-enhancement generate when the methods cannot sufficiently consider the assumption. Therefore, it is necessary to evaluate how much further the methods can consider the characteristics of reflectance and illumination. However, we can not obtain the ground truth for reflectance and illumination in actual applications. Thus, in order to confirm the effectiveness of the proposed method, the proposed method is compared with SRIE, WVM, and JieP because these methods are based on Retinex model and are implemented on HSV-color space as well as the proposed method.

Fig.4.2 summarizes the decomposition results of reflectance and illumination in different methods. SRIE cannot significantly distinguish between reflectance and illumination component, so that the estimated reflectance contains little textures detail. WVM sufficiently reveals textures detail in the estimated reflectance, but amplifies noise in dark regions. Moreover, the methods over-smooth illumination, so that the estimated reflectance generates halo artifacts in edges of buildings. JieP sufficiently removes illumination component from reflectance, but the estimated illumination loses the meaningful structure information too much. As a result, the estimated reflectance generates halo artifacts in edges of buildings. Moreover, the estimated reflectance contains much noise in dark regions. In summary, the proposed method can sufficiently maintain the structure information with less textures detail in the estimated illumination. In addition, the proposed method can reveal fine textures detail while suppressing halo artifacts, noise amplification, and over-enhancement in the estimated reflectance.



(a) SRIE



(b) WVM



(c) JieP



(d) Ours

Figure 4.2: Reflectance and illumination for different methods.((a)-(d) top: reflectance, bottom: illumination)

4.4 Qualitative Evaluation

This section focuses on the comparison based on the qualitative evaluation. In the qualitative evaluation, the discussion centers on whether the methods can enhance low-light images naturally and significantly. Similar to the above comparison of decomposition, several state-of-the-art methods are used: three Retinex methods including SRIE, WVM, and RRM; non-Retinex method (LIME).

Fig.4.3 summarizes the enhancement results of all the methods for dataset #6. The dataset #6 has two features. One is that the enhanced image usually generates halo artifacts in edges of buildings. The other is that the enhanced image tends to lose textures detail in the right tower which contains high intensities in the entire image. SRIE and WVM generate noticeable halo artifacts in the edges of the tower. In addition, these methods lose textures detail because these methods cannot significantly decompose the low-light image into reflectance and illumination and prevent the awareness of textures detail. RRM exhibits an outstanding performance in suppression of halo effects and contrast enhancement, but the result of this method is likely to be blurry and loses textures detail. LIME shows impressive performance in lighting up dark regions. However, the method often over-enhances the low-light image, so that the enhanced image loses textures detail too much, specifically in bright regions. In summary, the proposed method can suppress halo artifacts and over-enhancement. Moreover, the proposed method clarifies more textures detail even in bright regions.

Fig. 4.4 summarizes the enhancement results of all the methods for dataset #7. The dataset #7 has two features. One is that the over-enhances is usually caused in bright regions. The other is that noise tends to be amplified in dark regions. SRIE can naturally enhance the low-light image, but this method can not sufficiently help the awareness of textures detail. WVM satisfactorily enhances the low-light image, but generates severe noise amplification in dark regions. RRM performs image enhancement while suppressing noise amplification, but the generated image is too smooth and is over-enhanced on the entire image. LIME illuminates dark regions, but over-enhances bright regions. In summary, the proposed method achieves good performances in image enhancement, the awareness of textures detail, and suppression of noise amplification and over-enhancement.

4.5 Quantitative Evaluation

This section focuses on the comparison with the proposed method and several state-of-the-art methods in terms of two quantitative evaluations: lightness order error (LOE) [22] and autoregressive-based image sharpness metric (ARISM) [23]. The evaluations indicate naturalness of the enhanced image. The smaller the score of the evaluations are, the better an enhanced image preserves naturalness of lightness.

4.5.1 Lightness Order Error

As pointed out in [22], the relative order of lightness represents the light source directions and the lightness variation, since the naturalness of an enhanced image is related to the relative order of lightness in different local areas. LOE measures the lightness distortion



(a) Low-light Image



(b) SRIE



(c) WVM



(d) RRM



(e) LIME



(f) Ours

Figure 4.3: Comparison of low-light image enhancement results for test image #6.



(a) Low-light Image



(b) SRIE



(c) WVM



(d) RRM



(e) LIME



(f) Ours

Figure 4.4: Comparison of low-light image enhancement results for test image #7.

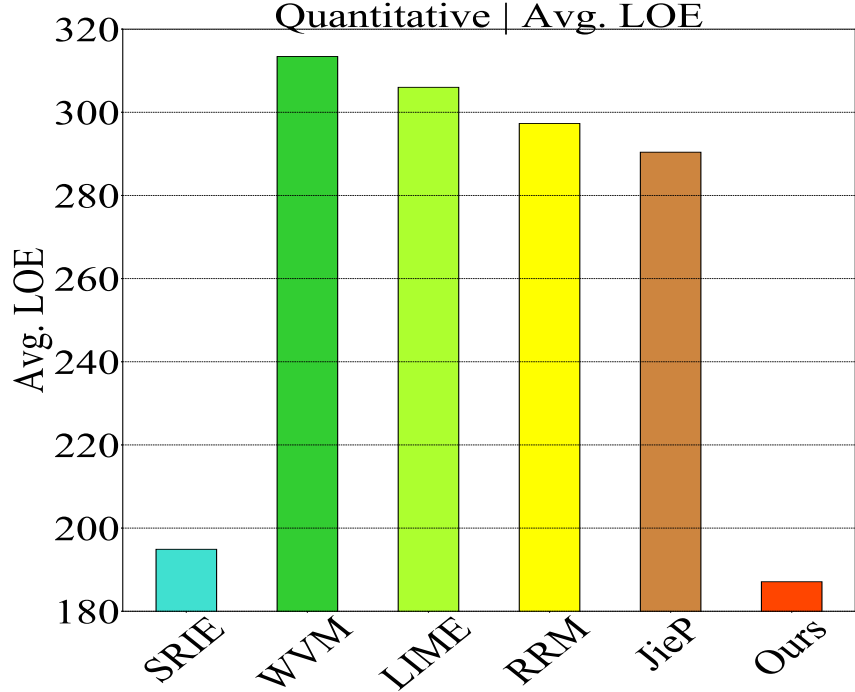


Figure 4.5: Comparison of the average score in the LOE for different methods.

of enhanced images as follows:

$$\text{LOE} = \frac{1}{m} \sum_{x=1}^m RD(x), \quad (4.1)$$

where m is the pixel number. Here $RD(x)$ is the relative order difference of the lightness between an observed image S and the enhanced image S' for pixel x , defined by

$$RD(x) = \sum_{y=1}^m F(B(x), B(y)) \oplus F(B'(x), B'(y)), \quad (4.2)$$

where \oplus stands for the exclusive-or operator, $B(x)$ and $B'(x)$ are the bright channel of an observed image and the enhanced image at the location x , respectively. The function $F(p, q)$ returns 1 if $q \in p$, 0 otherwise. As suggested in [10], down-sampling is needed to reduce the complexity of computing LOE. Therefore, when evaluating LOE, all images are down-sampled to 50×50 .

As shown in Fig. 4.5 and Table 4.1, the proposed method outperforms the others in almost all images. This means that the proposed method can keep the naturalness of images well when enhancing. The proposed method sufficiently suppresses halo artifacts, noise amplification and over-enhancement, since the proposed method incorporates the characteristics of reflectance and illumination with the optimization equation. In other words, the mixture $L_2 - L_P$ variational Retinex model and the adaptive texture map contribute to alleviation on such negative effects.

Table 4.1: The number of images in each rank based on LOEs.

Rank \ Method	SRIE	WVM	LIME	RRM	JieP	Ours
1st	6	0	2	1	0	12
2nd	10	1	3	2	0	5
3rd	2	3	1	5	8	2
Others	3	17	15	13	13	2

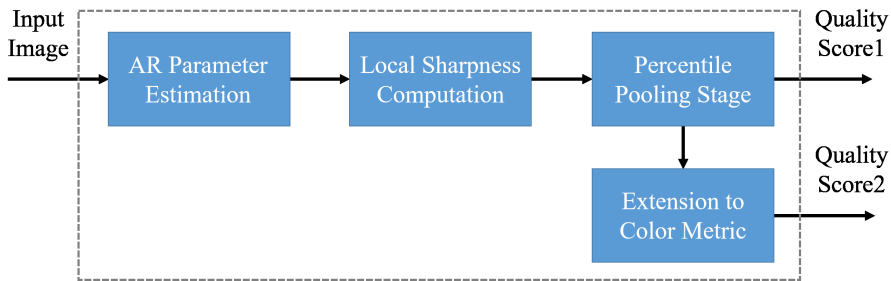


Figure 4.6: The number of images in each rank based on ARISMs.

4.5.2 Autoregressive-based image sharpness metric

ARISM is a blind sharpness measure via parameter analysis of classical autoregressive (AR) image model. The measure estimates the sharpness in the parameter space by analyzing the difference of the locally estimated AR parameters. Moreover, the measure is taken into account the inevitable influence of color information on the sharpness assessment by extending YIQ-color space. Fig. 4.6 shows the primary framework of ARISM, representing all procedures.

Fig. 4.7 and Tab. 4.2 summarize the results of ARISM. It can be seen that the proposed method achieves the lowest average performances among all methods. In addition, the proposed method is as versatile as RRM because both the methods show the better results in almost all images. This means that the proposed method can enhance low-light images while keeping image sharpness. Thus, the mixture $L_2 - L_p$ variational Retinex model and the texture map A_d have a good impact on preserving the salient structure information and revealing textures detail.

Table 4.2: The table represents the number of each rank in the values of ARISM of all images

Rank \ Method	SRIE	WVM	LIME	RRM	JieP	Ours
1st	3	1	0	8	0	9
2nd	4	9	0	3	2	3
3rd	5	5	1	2	7	1
Others	9	6	20	8	12	8

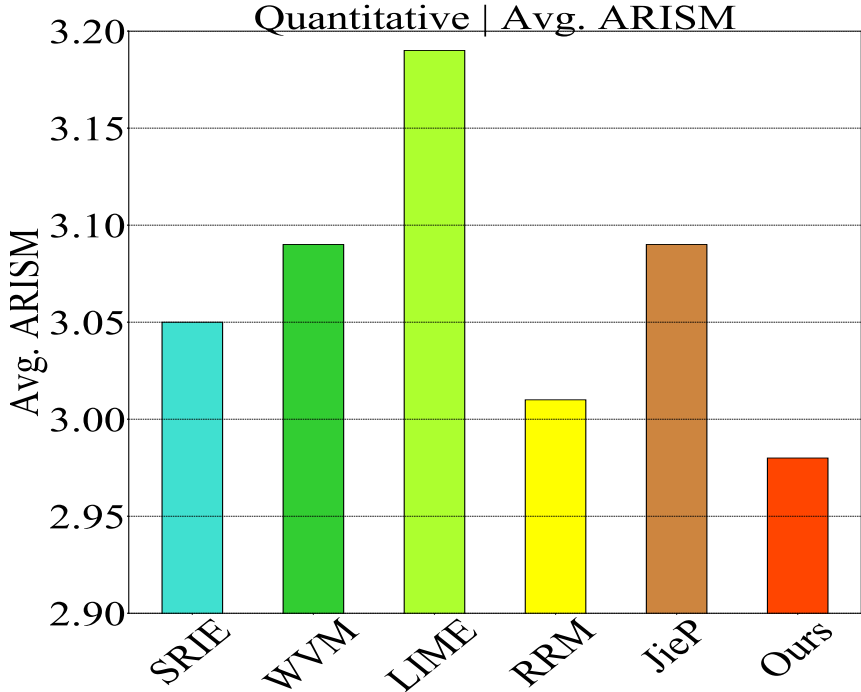


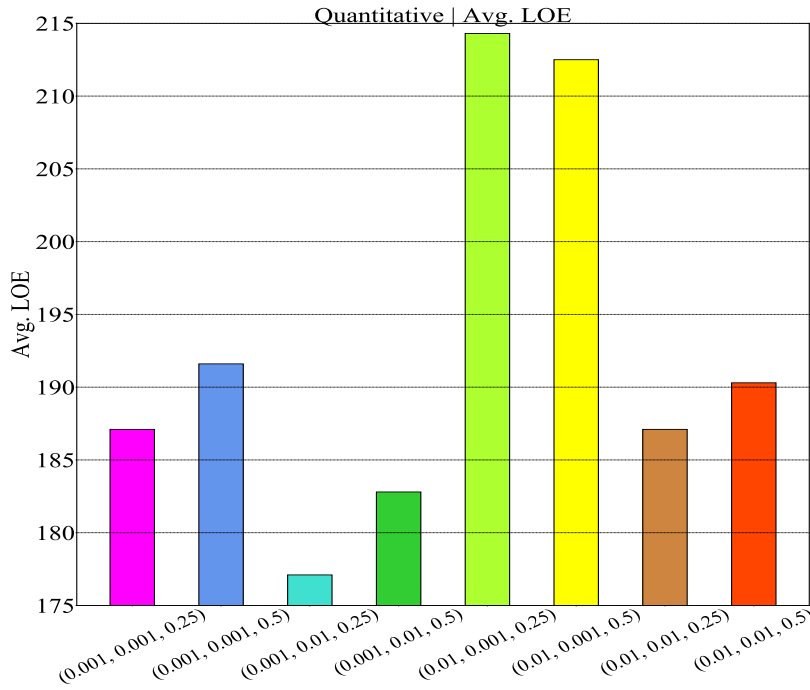
Figure 4.7: Comparison of the average score in the ARISMs for different methods.

4.6 Parameter Study

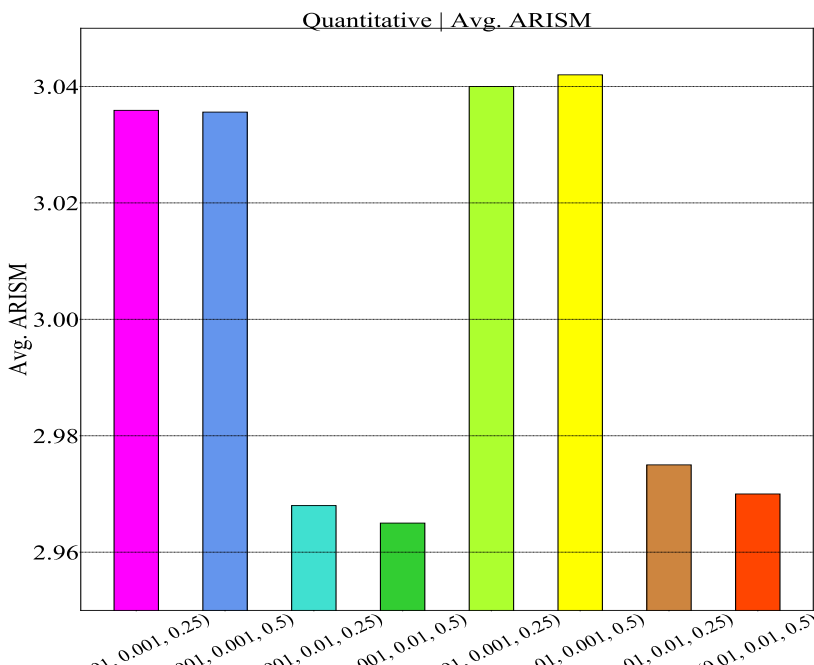
This section discusses on how to set the empirical parameters α , β , γ . The setting are performed with the both qualitative and quantitative evaluations described in Sec. 4.4 and 4.5. Please note again that lower LOE and ARISM values represent better visual quality.

In Fig. 4.8, we give objective results obtained with different (α, β, λ) pairs on all dataset images, where α and β are selected from either of 0.01 or 0.001, and γ is selected from either of 0.25 or 0.5. As can be observed, the parameter λ should be set to 0.25 because the choice of $\lambda = 0.25$ achieves lower LOEs than the choice of $\lambda = 0.5$, and they achieve almost the same ARISMs. Next, we can see that results with the choices of $(\alpha, \beta, \gamma) = (0.001, 0.001, 0.25)$, $(0.001, 0.01, 0.25)$, and $(0.01, 0.01, 0.25)$ achieve low LOEs. In addition, among them, the choices of $(0.001, 0.01, 0.25)$ and $(0.01, 0.01, 0.25)$ achieve low ARISMs and have almost the same ARISMs.

Fig. 4.9 demonstrates the qualitative comparisons of reflectance, illumination, and the enhanced images with different (α, β) pairs on dataset #5. As can be observed, the estimated illumination becomes smoother as α increases. The details of the estimated reflectance are weakened as β increases since the use of a larger β achieves stronger noise reduction. The details of the estimated reflectance are strengthened as α increases and β decreases, but such parameters lead to generation of noise and artifacts. Therefore, in these experiments, we set (α, β, γ) as $(0.01, 0.01, 0.25)$.



(a) Plot of average LOEs



(b) Plot of average ARISMs

Figure 4.8: Plots of average values on each evaluation in different parameters α, β, γ .

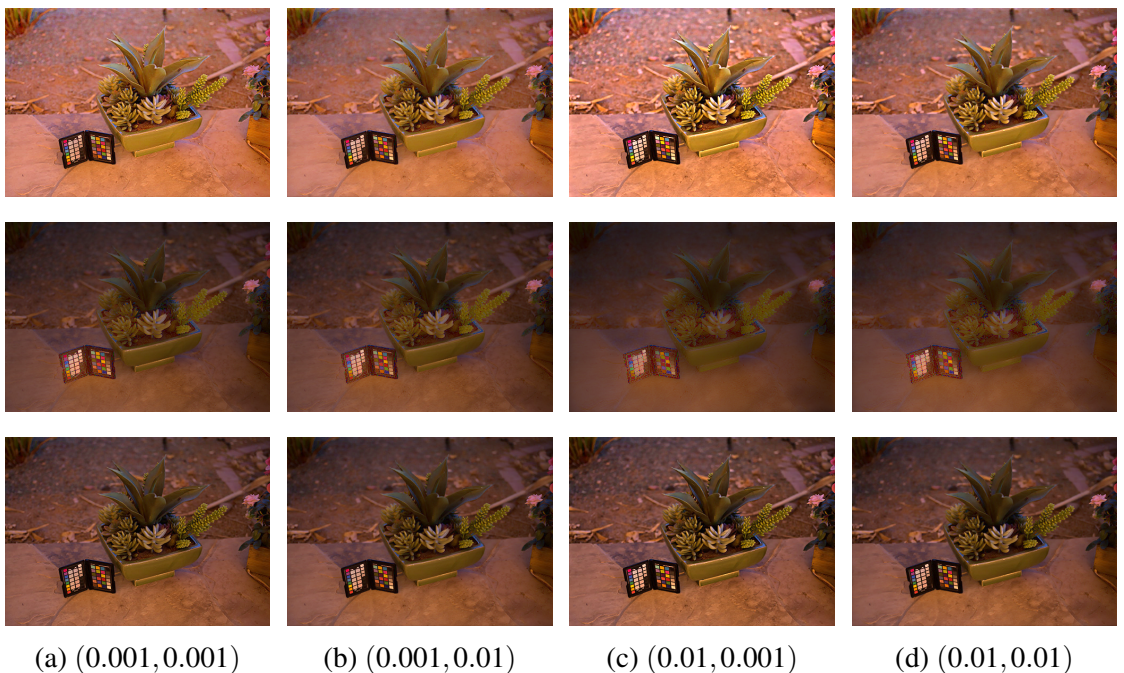


Figure 4.9: Results for different results of (α, β) pairs. Top: reflectance. Middle: illumination. Bottom: enhanced images.

Chapter 5

Conclusion

In this paper, we proposed a mixture $L_2 - L_p$ variational Retinex model with an adaptive texture map. First, we incorporated constraint terms on reflectance and illumination which further consider the characteristics of reflectance and illumination with a cost function of a minimization optimization problem. Next, we developed the adaptive texture map which is used to tune the noise reduction rate according to the brightness of an observed image. Moreover, the adaptive texture map contributes to reveal fine textures detail in the estimated reflectance. As the results, the proposed method can preserve texture details as much as possible while suppressing noise amplification and over-enhancement in the reflectance estimation, and smooth illumination as much as possible while keeping the structure information in the illumination estimation. Both qualitative and quantitative evaluations show that the proposed method can enhance low-light images more naturally than the state-of-the-art methods. In particular, in the LOE evaluation, the proposed method outperforms the other methods in almost all the images.

Acknowledgement

I would like to give heartfelt thanks to Prof. Youji Iiguni who provided fruitful suggestions and helpful comments and help in interpreting the significance of this study. I also appreciate to Associate Prof. Ryota Shimokura who provided helpful comments and suggestions in practical aspect. Finally, I would like to thank all the Bachelor, Master, Doctor students in Iiguni laboratory.

Reference

- [1] E. D. Pisano *et al*, “Contrast limited adaptive histogram equalization image processing to improve the detection of simulated speculations in dense mammograms,” *J. Digit. Image*, vol. 11, no. 4, pp. 193-200, 1998.
- [2] H. Cheng and X. Shi, “A simple and effective histogram equalization approach to image enhancement,” *Digital Signal Processing*, vol. 14, no. 2, pp. 158-170, 2004.
- [3] S.-C. Huang, F.-C. Cheng, and Y.-S. Chiu, “Efficient contrast enhancement using adaptive gama correction with weighting distribution,” *IEEE Trans. Image Process.*, vol. 20, no. 5, pp. 1262-1272, 2011.
- [4] L. Li, R. Wang, W. Wamg, and W. Gao, “A low-light image enhancement method for both denoising and contrast enlarging,” in *Proc. IEEE Int. Conf. Image Process.*, pp. 3730-3734, 2015.
- [5] X.Zhang, P.Shen, L. Luo, L. Zhang, and J. Song, “Enhancement and noise reduction of very low light level images,” in *Proc. 21st Int. Conf. Pattern Recognit. (ICPR)*, pp. 2034-2037, 2012.
- [6] D. J. Jobson, Z.-U. Rahman, and G. A. Woodell, “Properties and performance of a center/surround retinex,” *IEEE Trans. Image Process.*, vol. 6, no. 3, pp. 451-462, 1997.
- [7] D. J. Jobson, Z.-U. Rahman, and G. A. Woodell, “A multiscale retinex for bridging the gap between color images and the human observation of scenes,” *IEEE Trans. Image Process.*, vol. 6, no. 7, pp. 965-976, 1997.
- [8] X. Fu, Y. Liao, D. Zeng, Y. Huang, X. Zhang, and X. Ding, “A probabilistic method for image enhancement with simultaneous illumination and reflectance estimation,” *IEEE Trans. Image Process.*, vol. 24, no. 12, pp. 4965-4977, 2015.
- [9] X. Fu, D. Zeng, Y. Huang, X. Zhang and X. Ding, “A weighted variational model for simultaneous reflectance and illumination estimation,” *IEEE Conf. Computer Vis. Pattern Recognit.*, pp. 2782-2790, 2016.
- [10] X. Guo, Y. Li, and H. Ling, “LIME: Low-light image enhancement via illumination map estimation,” *IEEE Trans. Image Process.*, vol. 26, no. 2, pp. 982-993, 2017.
- [11] B. Cai, X. Xu, K. Guo, K. Jia, B. Hu, and D. Tao, “A joint intrinsic-extrinsic prior model for retinex,” In *Proc., IEEE Conf. Computer Vis., Pattern Recognit.*, pp. 4000-4009, 2017.

- [12] M. Li, J. Liu, W. Yang, X. Sun, and Z. Guo, “Structure-revealing low-light image enhancement via robust Retinex model,” *IEEE Trans. Image Process.*, vol. 27, no. 6, pp. 2828-2841, 2018.
- [13] E. H. Land and J. J. McCann, “Lightness and retinex theory,” *J. Opt. Soc. Amer.*, vol. 61, no. 1, pp. 1-11, 1971.
- [14] K. He, J. Sun, and X. Tand, “Guided image filtering,” *Proc. European Conf. on Computer Vis.*, pp. 1-14, 2010.
- [15] C. Fu, L. Duan, and C. Xiao, “A hybrid L₂-L_p variational model for single low-light image enhancement with bright channel prior,” *IEEE Int. Conf. on Image Process. (ICIP)*, 2019.
- [16] N. Bonneel, B. Kovacs, S. Paris, and K. Bala, “Intrinsic decompositions for image editing,” *Computer Graphics Forum*, vol.36, no. 2, 2017.
- [17] P. Tseng, “Convergence of a block coordinate descent method for nondifferentiable minimization,” *Journal of Optimization Theory and Applications*, vol. 109, no. 3, pp. 475-494, 2001.
- [18] E. J. Candès, M. B. Wakin, and S. P. Boyd, “Enhancing sparsity by reweighted l_1 minimization,” *Journal of Fourier Analysis and Applications*, vol. 14, no. 5-6, pp. 877-905, 2008.
- [19] L. Xu, S.Zheng, and J. Jia, “Unnatural 10 sparse representation for natural image deblurring,” *IEEE Conf. Computer Vis. Pattern Recognit.*, pp. 1107-1114, 2013.
- [20] X. Fu, D. Zheng, Y. Huang, X. Ding, and X-P. Zhang, “A variational framework for single low light image enhancement using bright channel prior,” in *Proc. IEEE Global Conf. on Signal and Inform. Process.*, pp. 1085-1088, 2013.
- [21] S. Park, S. Yu, B. Moon, S. Ko, and J. Paik, “Low-light image enhancement using variational optimization-based retinex model,” *IEEE Trans. on Cons. Elec.*, vol. 63, no. 2, pp. 178-184, 2017.
- [22] S. Wang, J. Zheng, H.-M. Hu, and B. Li, “Naturalness preserved enhancement algorithm for non-uniform illumination images,” *IEEE Trans. Image Process.*, vol. 22, no. 9, pp. 3538-3578, 2013.
- [23] K. Gu, G. Zhai, W. Lin, X. Yang, and W. Zhang, “No reference image sharpness assessment in autoregressive parameter space,” *IEEE Trans. on Image Process.*, vol. 24, no. 10, pp. 3218-3231, 2015.

Publication

International Conference

- Kazuki Kurihara, Hiromi Yoshida, and Youji Iiguni, "Low-Light Image Enhancement via Adaptive Shape and Texture Prior", Proc. of 15th International Conference on Signal Image Technology & Internet Based Systems (SITIS 2019), pp. 74-81, Nov. 2019.

Domestic Conference

- 粟原一樹, 吉田大海, 飯國洋二, "Variational Retinex Model と活性化マップを用いた夜間低照度画像の鮮明化", 画像電子学会 第286回研究会, Aug. 2018.